

# A pH-Responsive Carrier System that Generates NO Bubbles to Trigger Drug Release and Reverse P-Glycoprotein-Mediated Multidrug Resistance\*\*

Ming-Fan Chung, Hung-Yi Liu, Kun-Ju Lin, Wei-Tso Chia,\* and Hsing-Wen Sung\*

**Abstract:** Multidrug resistance (MDR) resulting from the overexpression of drug transporters such as P-glycoprotein (Pgp) increases the efflux of drugs and thereby limits the effectiveness of chemotherapy. To address this issue, this work develops an injectable hollow microsphere (HM) system that carries the anticancer agent irinotecan (CPT-11) and a NO-releasing donor (NONOate). Upon injection of this system into acidic tumor tissue, environmental protons infiltrate the shell of the HMs and react with their encapsulated NONOate to form NO bubbles that trigger localized drug release and serve as a Pgp-mediated MDR reversal agent. The site-specific drug release and the NO-reduced Pgp-mediated transport can cause the intracellular accumulation of the drug at a concentration that exceeds the cell-killing threshold, eventually inducing its antitumor activity. These results reveal that this pH-responsive HM carrier system provides a potentially effective method for treating cancers that develop MDR.

**R**ecent research in chemotherapy has strongly prioritized the mitigation of the multidrug resistance (MDR) effect in cancer cells.<sup>[1]</sup> The MDR of cancer cells arises from the overexpression of their plasma-membrane P-glycoprotein (Pgp) transporters, which actively increases the drug efflux and limits the effectiveness of anticancer agents.<sup>[2]</sup> Accordingly, a method that greatly improves intracellular drug accumulation and the sensitivity of MDR tumor cells to drugs is urgently required.

It has been suggested that the resistance of cancer cells to chemotherapeutics can be reversed by exposure to nitric

oxide (NO), a gaseous molecular messenger that can reduce their Pgp expression levels.<sup>[3]</sup> However, the use of NO as a therapeutic agent is limited by its gaseous state and extremely short half-life.<sup>[4]</sup> Therefore, developing a carrier system that contains an NO-releasing donor that supports the controlled and prolonged release of NO to modulate the reversal of Pgp-mediated MDR is a serious challenge.

To achieve this goal, this work develops an injectable hollow-microsphere (HM) system that carries the anticancer agent irinotecan (CPT-11) and the NO-releasing donor diethylenetriamine diazeniumdiolate (DETA NONOate) in its hydrophilic core.<sup>[5]</sup> Such a HM system can produce NO bubbles in the acidic environment of tumor tissues to trigger localized drug release and reverse the Pgp-mediated MDR in cancer cells. The combination of increased glucose metabolism and poor perfusion yields an acidic extracellular pH of 6.5–6.9 in malignant tumors, whereas normal tissues have a physiological pH of 7.2–7.4.<sup>[6]</sup> The shell of HMs is fabricated from poly(D,L-lactic-co-glycolic acid) (PLGA), which is widely used as a drug-carrier material.<sup>[7]</sup> DETA NONOate (NONOate) decomposes by hydrolysis at acidic pH, releasing two NO molecules.<sup>[8]</sup> CPT-11, a camptothecin derivative, has been utilized to treat various cancers, including breast cancer; nevertheless, this molecule suffers from Pgp-induced efflux.<sup>[9]</sup>

Figure 1 depicts the structure/composition of this HM carrier system and the mechanism by which it treats CPT-11-resistant breast cancer cells (MCF-7/ADR) that are generated subcutaneously in a nude mouse model. Upon injection into an acidic tumorous environment, the NONOate that is encapsulated in the HMs reacts with acid to form NO bubbles, producing permeable defects in their PLGA shells, causing the release of CPT-11 to a local target that is adjacent to the tumor cells. As well as having a critical role in triggering drug release, the formed NO may act as a Pgp-mediated MDR reversal agent in tumor cells. By reversing the MDR effect, the released CPT-11 accumulates in the tumor cells in an amount that exceeds the therapeutic threshold,<sup>[10]</sup> eventually leading to antitumor activity.

To deliver and release effectively large quantities of drugs in a highly localized and controlled manner in specific areas, NONOate and CPT-11 were encapsulated in the HM carrier system. Test HMs were prepared from PLGA using a microfluidic device in water-in-oil-in-water (W/O/W) double emulsions. In this experiment, the inner water phase was an aqueous solution of NONOate and CPT-11 at pH 8.0, the middle oil phase was PLGA in dichloromethane, and the outer water phase was a surfactant solution of poly(vinyl alcohol) (PVA). To prevent hydrolysis, NONOate is typically stored in an alkaline buffer at pH 8.0.<sup>[8]</sup>


[\*] M.-F. Chung,<sup>[†]</sup> H.-Y. Liu,<sup>[†]</sup> Prof. H.-W. Sung  
Department of Chemical Engineering and Institute of Biomedical Engineering, National Tsing Hua University  
Hsinchu, Taiwan (ROC)  
E-mail: hwsung@mx.nthu.edu.tw

Dr. K.-J. Lin  
Department of Nuclear Medicine and Molecular Imaging Center  
Chang Gung Memorial Hospital, Taoyuan, Taiwan (ROC)

Dr. W.-T. Chia  
Department of Orthopaedics, National Taiwan University Hospital  
Hsinchu Branch, Hsinchu, Taiwan (ROC)  
E-mail: 4926602@yahoo.com.tw

[†] These authors contributed equally to this work.

[\*\*] This work was supported by a grant from the National Science Council (NSC 101-2320-B-007-003-MY3), Taiwan (ROC). The PET imaging study was supported by grants from Chang Gung Memorial Hospital at Linkou (CMRPG300161 and CMRPG391513), Taiwan.

 Supporting information (including experimental materials and methods) for this article is available on the WWW under <http://dx.doi.org/10.1002/anie.201504444>.

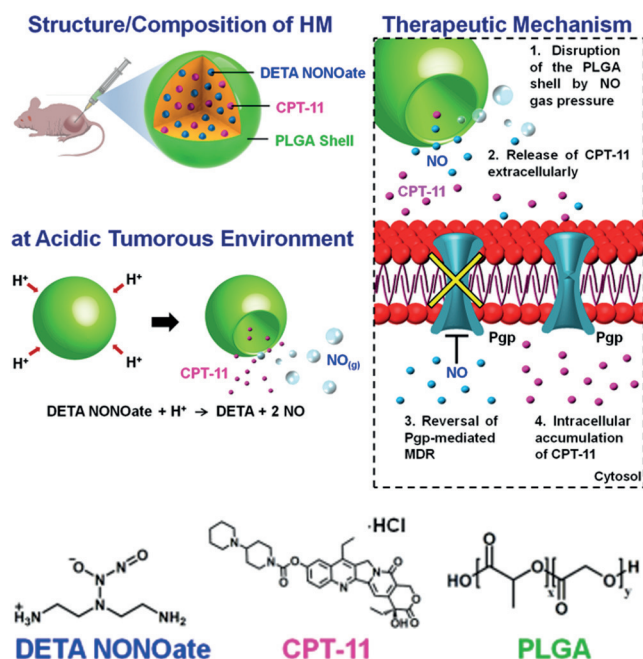


**Figure 1.** Schematic structure/composition of HMs developed herein and their mechanism in the treatment of MDR tumors.

Figure 2a shows photomicrographs of the resultant HMs following the evaporation of dichloromethane. The HMs were monodisperse with a polydispersity of about 3 %, and had a diameter of  $387.1 \pm 11.7 \mu\text{m}$  and a shell thickness of  $24.5 \pm 2.4 \mu\text{m}$  ( $n = 6$  batches). The NONOate ( $48.5 \pm 1.2 \mu\text{g mg}^{-1}$ ) and CPT-11 ( $3.2 \pm 0.5 \mu\text{g mg}^{-1}$ ) contents in HMs were determined by UV/Vis absorption spectroscopy after the HMs had been broken by sonication.

The sensitivity of HMs to the pH value was studied in media with pH values of 8.0, 7.4, and 6.6, to mimic their

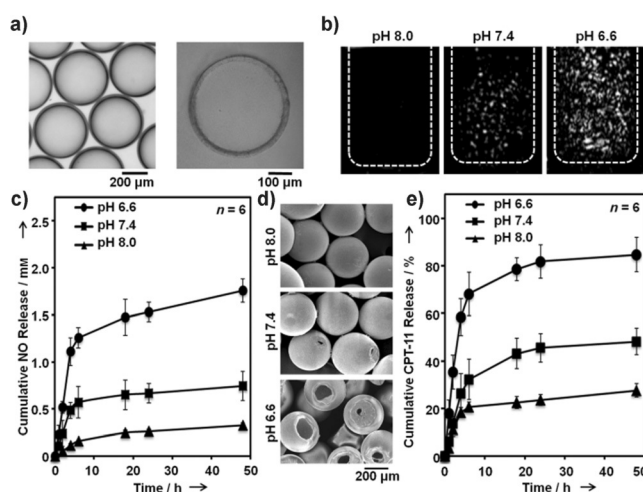


**Figure 2.** a) Photomicrographs of test HMs and a representative frozen cross-section of one HM. Properties of HMs that were immersed in phosphate-buffered saline (PBS) with various pH values at  $37^\circ\text{C}$ : b) ultrasound images showing the generation of NO bubbles, c) release profiles of NO, d) SEM micrographs showing the morphology of the test HMs following the experiment, and e) the release profiles of CPT-11.

storage conditions and the extracellular environments of tumors and normal tissues, respectively. NONOate hydrolyzes in a pH-dependent manner.<sup>[11]</sup> In an acidic environment, protons can infiltrate the PLGA shell of HMs and react with their encapsulated NONOate to form NO bubbles that are hyperechogenic and can be detected using an ultrasound imaging system. Figure 2b reveals that at pH 8.0, the HMs generated no bubbles, whereas at pH 7.4, a few NO bubbles were detected in the sample. At pH 6.6, many NO bubbles were formed by the HMs in the first 6 h of reaction and, over the subsequent 42 h, NO continued to be produced but in a smaller amount (Figure 2c; the original data are tabulated in Table S2 in the Supporting Information). When the pressure of NO reached a certain level, the PLGA shells of the HMs were disrupted and pores were formed therein (Figure 2d), resulting in the local unloading of the encapsulated CPT-11.

Figure 2e (see Table S3 for the tabulated original data) displays the CPT-11 release profiles of the test HMs in environments with various pH values. At pH 8.0, a rapid, initial release of the drug concentration was detected. This effect can be regarded as a burst effect that is attributable mainly to the weak binding of the drug to the relatively large surfaces of the HMs. The subsequent release of CPT-11 from HMs was minimal, suggesting that the HMs were relatively stable when stored. As the environmental pH was decreased, the HMs released significant amounts of CPT-11, yielding a high local drug concentration. Notably, the percentage of CPT-11 that was released from the HMs was considerably greater at pH 6.6 (circa 85 %) than at pH 7.4 (circa 45 %), revealing that the developed HM system may respond to the small difference in pH value between normal and tumor tissues.

The effects of the developed HMs on the reversal of the Pgp-mediated MDR in MCF-7/ADR cells were then studied in vitro at pH 7.4 and 6.6, to mimic the pH environments of normal and tumor tissues, respectively. The inhibition of the expression of Pgp was investigated by immunofluorescence staining and flow cytometry. The intracellular accumulation of CPT-11 was analyzed using high-performance liquid chromatography (HPLC) after lysis of the cells, and the cell viability was evaluated using a live/dead staining method and the MTT assay (MTT = 3-(4,5-dimethylthiazol-2-yl)-2,5-diphenyltetrazolium bromide). In these experiments, MCF-7/ADR cells were incubated using test HMs ( $4 \text{ mg mL}^{-1}$ , containing  $1.0 \text{ mM}$  NONOate and  $20 \mu\text{M}$  CPT-11; see the Supporting Information for a brief discussion) for 24 h.

The MDR cells that received the HMs that were exposed to pH 7.4 exhibited only a slightly different inhibition of Pgp expression (circa 10 % inhibition), accumulation of CPT-11 (circa 13 % higher), and viability (circa 5 % lower) compared to those of the untreated control group (Figure 3a,b,d,e) or that received free CPT-11 (Figure 3c). In contrast, the cells that were treated with the HMs at pH 6.6 exhibited a significantly reduced Pgp expression level (approximately 45 % reduction), and therefore a significantly larger amount of intracellularly accumulated CPT-11 (circa 100 % increase), and a lower cell viability (circa 50 % decrease). Notably, pH value did not significantly affect the viability of cells in the

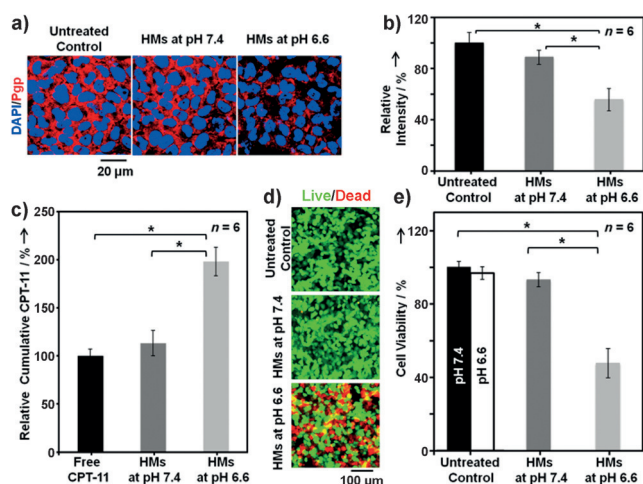


**Figure 3.** Reversal of Pgp-mediated MDR in MCF-7/ADR cells using test HMs at different pH environments: a) confocal images of Pgp expression levels and b) quantitative results of flow cytometric analysis, c) intracellular accumulations of CPT-11 obtained by HPLC analysis, d) fluorescence images of the viability of the treated cells, and e) quantitative results obtained by the MTT assay. \*Statistical significance at  $P < 0.05$ . DAPI = 4',6-diamidino-2-phenylindole.

untreated control group over the studied pH range. These experimental results show that the pH-responsive HMs that were developed herein effectively reversed Pgp-mediated MDR and increased the accumulation of the drug in cancer cells, ultimately improving the sensitivity of tumor cells to drugs. The correct and careful design of a drug carrier that can distinguish between a tumor and normal tissue is critical to improving treatment efficacy.<sup>[12]</sup>

The capacity of the developed HMs to distinguish between the in vivo environments of normal and tumor tissues was examined in nude mice by examining their in vivo drug-release behavior. To produce the animal model, the right sides of the backs of mice were subcutaneously implanted with MCF-7/ADR cells to form tumors, whereas the left sides of their backs were left untreated to provide normal tissues. To monitor the release behavior of the HMs, a hydrophilic cyanine-based fluorescent dye (Cy5) was loaded into the HMs as a model drug, because no fluorescence was detected from CPT-11. The HMs that contained NONOate/Cy5 were separately injected into the normal and tumor-bearing backs. The fluorescence intensities of Cy5 were then measured using an in vivo imaging system (IVIS). Theoretically, when Cy5 is within HMs at high concentrations, its fluorescence signal is quenched, and its fluorescence intensity increases considerably upon release through the shell.<sup>[13]</sup> At high concentrations, aggregates of fluorescence molecules begin to appear and act as trapping sites for the excitation energy.<sup>[14]</sup>

As shown in Figure 4a and 4b, weak Cy5 fluorescence emission was detected from both sides of the backs of the mice immediately following the initial injection (0 h). The fluorescence intensity from the left sides (normal tissue) changed only slightly within the first 6 h of treatment with the test HMs, suggesting that the release of Cy5 from HMs was slow in normal tissues. In contrast, the increase in the

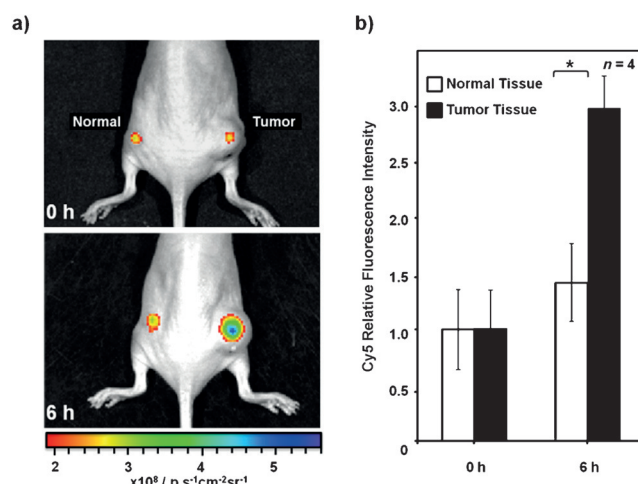


**Figure 4.** In vivo drug release behaviors of HMs that were intratumorally injected into normal and tumor tissues: a) Cy5 fluorescence signals detected by IVIS and b) their relative fluorescence intensities. \*Statistical significance at  $P < 0.05$ .

fluorescence intensity by a factor of approximately three over a large area on the right sides of the backs (tumor tissue) over time ( $P < 0.05$ ) revealed that the HMs that were injected into the tumor tissues were triggered to release effectively the Cy5, probably because of the increased acidity of the environment in tumor cells. The measured difference between fluorescence intensities verifies that the HMs that were developed herein effectively differentiated between normal and tumor tissues and so may be useful as a drug delivery system in the treatment of cancer.

Finally, the antitumor efficacy of the developed HMs was investigated in nude mice with subcutaneous MCF-7/ADR xenograft tumors following their intratumoral injection. The group with no treatment (untreated control) and the groups that received free CPT-11 or free NONOate/CPT-11 were the controls.

Relative to the untreated control group, the free CPT-11 group exhibited minimal antitumor activity against the MDR tumors (Figure 5a). The groups that had been treated with free NONOate/CPT-11 or the HMs that contained NONOate/CPT-11 exhibited significantly suppressed tumor volume. Notably, the antitumor capacity of the NONOate/CPT-11 HMs exceeded that of the NONOate/CPT-11 in free form ( $P < 0.05$ ). Body weight was reduced only in the groups that received free CPT-11 or free NONOate/CPT-11 ( $P < 0.05$ ), reflecting a general toxicity (Figure 5a, right).

As NONOate and CPT-11 are both water-soluble compounds, they may readily migrate away from the tumor tissue before releasing NO when injected intratumorally, with negative side effects. As demonstrated in the in vitro study (Figure 2), the NONOate that was encapsulated in HMs had to decompose to generate a sufficient gas pressure to disrupt the PLGA shell before locally releasing NO and CPT-11. Therefore, the amounts of NO and CPT-11 that accumulated at the tumor site in the group that was treated with the HMs significantly exceeded those in the group that had been treated with free NONOate/CPT-11. The NO-reduced Pgp-mediated transport and the site-specific CPT-11 release then

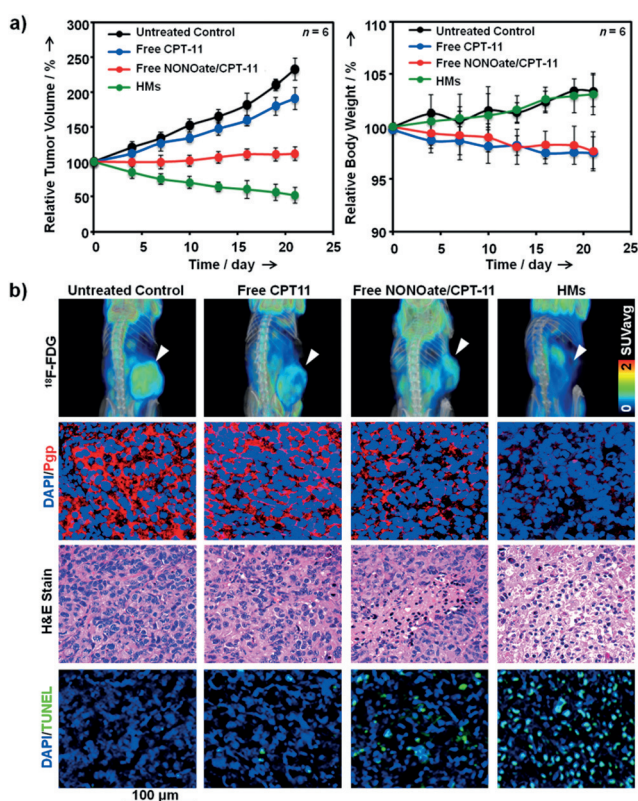


**Figure 5.** a) Changes in relative tumor volume and body weight of mice with MCF-7/ADR tumors in response to various treatments. b) Results demonstrating the antitumor efficacy of each treatment modality on MDR tumors, showing (from top to bottom): PET images, Pgp expression levels, H&E staining, and TUNEL staining. H&E = hematoxylin and eosin; TUNEL = terminal deoxynucleotidyl transferase dUTP nick end labeling.

resulted in the accumulation of the drug at an intracellular concentration that was greater than the cell-killing threshold, resulting in greater cell death as a result of NO release than for CPT-11 release.

Toward the end of the treatments, the antitumor capacity of HMs against the implanted MDR cells was further quantified by positron emission tomography (PET) and by performing histological and immunofluorescence analyses of tumor sections. [ $^{18}\text{F}$ ]-fludeoxyglucose ([ $^{18}\text{F}$ ]-FDG) has been widely used as a PET contrast agent in tumor examinations. Increased FDG uptake typically reveals the high metabolic/proliferative activity of tumor tissues.<sup>[15]</sup>

Figure 5b indicates that the tumor average standard uptake value (SUVavg) of FDG in the group that received HMs ( $0.57 \pm 0.15$ ;  $n = 4$  per group) was significantly lower than those in the untreated control group ( $1.23 \pm 0.08$ ,  $P < 0.05$ ) and in the groups that received free CPT-11 ( $1.18 \pm 0.10$ ,  $P < 0.05$ ) or free NONOate/CPT-11 ( $0.81 \pm 0.11$ ,  $P < 0.05$ ). Furthermore, the results of the histological study demonstrate that the expression of Pgp in tumor tissues that had been treated with HMs was considerably suppressed below those of the other control groups, yielding signs of significant cell destruction, including a remarkable drop in the number of

cancerous cells (H&E stain) and the presence of many TUNEL-positive (green fluorescence) cells. These empirical data show that HMs that contain NONOate/CPT-11 are the most efficient method among all studied formulations for inhibiting the proliferation and inducing the apoptosis of MDR tumor cells. Therefore, this pH-responsive HM carrier system provides a potentially effective method for treating cancers that develop MDR.

**Keywords:** antitumor agents · cancer · drug delivery · fluorescence microscopy · multidrug resistance

**How to cite:** *Angew. Chem. Int. Ed.* **2015**, *54*, 9890–9893  
*Angew. Chem.* **2015**, *127*, 10028–10031

- [1] C. J. Ke, W. L. Chiang, Z. X. Liao, H. L. Chen, P. S. Lai, J. S. Sun, H. W. Sung, *Biomaterials* **2013**, *34*, 1.
- [2] Z. Wang, Z. Wang, D. Liu, X. Yan, F. Wang, G. Niu, M. Yang, X. Chen, *Angew. Chem. Int. Ed.* **2014**, *53*, 1997; *Angew. Chem.* **2014**, *126*, 2028.
- [3] a) C. Riganti, E. Miraglia, D. Viariso, C. Costamagna, G. Pescarmona, D. Ghigo, A. Bosia, *Cancer Res.* **2005**, *65*, 516; b) D. L. Anastasia, M. Noemi, S. Annalucia, P. Alessandra, P. Anna, Z. P. Jens, P. Raffaele, G. F. Maria, P. Pasquale, M. Gabriella, *Biochem. J.* **2011**, *440*, 175.
- [4] L. J. Ignarro, C. Napoli, J. Loscalzo, *Circ. Res.* **2002**, *90*, 21.
- [5] a) K. Takasuna, T. Hagiwara, M. Hirohashi, M. Kato, M. Nomura, E. Nagai, T. Yokoi, T. Kamataki, *Cancer Res.* **1996**, *56*, 3752; b) J. W. Yoo, E. S. Choe, S. M. Ahn, C. H. Lee, *Biomaterials* **2010**, *31*, 552.
- [6] V. Estrella, T. Chen, M. Lloyd, J. Wojtkowiak, H. H. Cornnell, A. I. Hashim, K. Bailey, Y. Balagurunathan, J. M. Rothberg, B. F. Sloane, *Cancer Res.* **2013**, *73*, 1524.
- [7] M. F. Chung, W. T. Chia, H. Y. Liu, C. W. Hsiao, H. C. Hsiao, C. M. Yang, H. W. Sung, *Adv. Healthcare Mater.* **2014**, *3*, 1854.
- [8] H. A. Hassanin, L. Hannibal, D. W. Jacobsen, M. F. El-Shahat, M. S. Hamza, N. E. Brasch, *Angew. Chem. Int. Ed.* **2009**, *48*, 8909; *Angew. Chem.* **2009**, *121*, 9071.
- [9] Y. Takashima, J. Hashimoto, Y. Kitamura, S. Shimma, Y. Fujiwara, F. Koizumi, K. Tamura, A. Hamada, *Cancer Res.* **2014**, *74*, 1678.
- [10] H. Wang, H. Xie, J. Wu, X. Wei, L. Zhou, X. Xu, S. Zheng, *Angew. Chem. Int. Ed.* **2014**, *53*, 11532; *Angew. Chem.* **2014**, *126*, 11716.
- [11] See Ref. [5b].
- [12] K. J. Chen, E. Y. Chaung, S. P. Wey, K. J. Lin, F. Cheng, C. C. Lin, H. L. Liu, H. W. Tseng, C. P. Liu, M. C. Wei, *ACS Nano* **2014**, *8*, 5105.
- [13] W. L. Chiang, Y. C. Hu, H. Y. Liu, C. W. Hsiao, R. Sureshbabu, C. M. Yang, M. F. Chung, W. T. Chia, H. W. Sung, *Small* **2014**, *10*, 4100.
- [14] a) W. J. Shi, J. Barber, Y. Zhao, *J. Phys. Chem. B* **2013**, *117*, 3976; b) B. E. Hardin, E. T. Hoke, P. B. Armstrong, J. H. Yum, P. Comte, T. Torres, J. M. J. Fréchet, M. K. Nazeeruddin, M. Grätzel, M. D. McGehee, *Nat. Photonics* **2009**, *3*, 406; c) C. J. Mu, D. A. Lavan, R. S. Langer, B. R. Zetter, *ACS Nano* **2010**, *4*, 1511.
- [15] S. Maschauer, J. Einsiedel, R. Haubner, C. Hocke, M. Ocker, H. Hübner, T. Kuwert, P. Gmeiner, O. Prante, *Angew. Chem. Int. Ed.* **2010**, *49*, 976; *Angew. Chem.* **2010**, *122*, 988.

Received: May 16, 2015

Published online: July 1, 2015